

Published Paper available here: <https://doi.org/10.1016/j.polymertesting.2015.06.010>

Ben Alcock, Jens Kjær Jørgensen, *The mechanical properties of a model hydrogenated nitrile butadiene rubber (HNBR) following simulated sweet oil exposure at elevated temperature and pressure*, Polymer Testing, Volume 46, 2015, Pages 50-58.

The mechanical properties of a model hydrogenated nitrile butadiene rubber (HNBR) following simulated sweet oil exposure at elevated temperature and pressure

Ben Alcock, Jens Kjær Jørgensen

### **Abstract**

A typical carbon black reinforced hydrogenated nitrile butadiene rubber (HNBR) was exposed to a mix of hydrocarbons (toluene, heptane and cyclohexane) at elevated temperatures and pressure in order to chemically age the material. The effect of this exposure on the mechanical properties is reported; the most significant change is a dramatic increase in tensile stiffness for specimens exposed at 160°C for 12 weeks. Differential scanning calorimetry (DSC) and dynamic mechanical thermal analysis (DMTA) revealed changes in the glass transition behaviour of this material, with a general reduction in the magnitude of the glass transition with increasing ageing time. In addition, gravimetric studies of the swollen specimens after removal from the hydrocarbon mix showed that the more aged specimens underwent significantly slower drying rates compared to less aged specimens. These results may be explained by an increase in crosslink density in the materials being the main mechanism occurring during chemical ageing of these HNBR compounds.

### **1. Introduction**

Hydrogenated nitrile butadiene rubbers (HNBRs) are well known for their resistance to chemical and thermal degradation, and can be formulated with varying acrylonitrile contents and degrees of hydrogenation. HNBRs find many applications which combine relatively high temperatures with exposure to petroleum products, such as automotive engine bay applications and sealing and piping equipment for the oil industry. In both of these application areas, high pressures and temperatures approaching 200°C create an aggressive environment for polymers, with peak engine bay temperatures predicted to increase in future [1] and deeper, more challenging subsea oilfield locations being targeted for future exploitation [2]. Research into the ageing of polymers during exposure to such conditions is, therefore, of great importance, but it is widely reported that degradation of HNBRs generally occurs through processes of chain scission and crosslinking; the former leading to a reduction in chain length typically manifested by reduction in tensile strength and strain to failure, and the latter resulting in a tighter network structure and evident from increasing stiffness [3-5]. As with any crosslinked polymer, the deformation response of the material is determined by both chemical crosslinks (due to chemical bonding between neighbouring polymer chains) and physical crosslinks (such as those due to molecular entanglements). Physical crosslinking due

to chain entanglements is dependent on molecular chain length, hence degradation processes which include chain scission would decrease the degree of physical crosslinking. Therefore, if both chain scission and the formation of new chemical crosslinks are expected during an ageing process, these can have opposing and compensating effects on the measured mechanical performance. The presence of fillers such as carbon black further complicate the mechanics of the system, as the behaviour local to filler particles is highly heterogeneous with chemical bonding between the filler and the polymer, and physical entrapment of polymer in the irregular geometry of filler aggregates restricting molecular mobility still further[6]. Because of the variety of overlapping effects which can restrict molecular movement in similar ways, the sum of these crosslinking phenomena can be collectively referred to as the apparent crosslinking.

Numerous authors have presented studies describing the ageing behaviour of various (often unfilled) nitrile butadiene rubbers either in hot air [5, 7-13] or in chemical environments [14-17]. The ISO 23936-2 and the related standard NORSOK M710 describe accelerated ageing tests to simulate ageing processes in elastomers by using increased temperatures to reduce test duration, and also suggest different chemical environments that may be used to simulate industry relevant chemical exposures. Prior to testing, a limit of acceptability is defined, typically a change in a mechanical characteristic or volume. Following the accelerated ageing, the specimens are considered to have passed or failed the acceptability test, depending on whether the predetermined criteria were satisfied. With this information, predictions can be made about how the materials would have performed if they had been tested at lower temperatures for longer times. As with all ageing predictions based on accelerating conditions, it must be assured that the same processes are occurring in the different test environments and various methods are reported for the verification of this [18]. Of course, accelerated ageing tests are only one part of a material qualification for a given application, and it is critical that the change in property that is used for the acceptability criteria is appropriate for the final application.

Ultimately, the most suitable chemical environment for assessing the ageing behaviour of HNBRs, or any other polymer, is the chemical environment that it will be exposed to in the final application. Where the chemical environment is well defined, dedicated exposure tests may be performed (for example, in a closed automotive engine system application using specified lubricants). However, in oilfield applications, there is some variation in the chemicals expected between one geographical site and another [19], and perhaps also over time within a single oilfield. The assessment of materials in large numbers of different oil simulating chemistries as part of the material qualification is unrealistic, and so standardized exposure liquid are usually applied. Because the goal of such ageing tests are material qualification, the results from such tests are rarely analysed further than the acceptability criteria for the particular test, and seldom presented in the academic community.

In this paper, a carbon black filled HNBR formulation was selected to represent a typical industrial formulation. This HNBR was then exposed to a sweet chemical environment suggested by ISO 23936-2 designed to approximate the aliphatic, aromatic and naphthenic hydrocarbons that are typically present in a subsea oil processing applications, at elevated pressure and at a range of temperatures. Although some oilfields also include varying degrees of concentrated hydrogen sulphide (H<sub>2</sub>S) gas, which is reported to attack HNBRs, this paper presents results on a simplified system without the inclusion of H<sub>2</sub>S. These results do not represent a particular commercial material formulation or application, but the results may be considered representative of similar materials. Following varying degrees of exposure, the mechanical properties were assessed by static tensile and dynamic torsional testing, hardness testing and a comparison of glass transition temperature measurements using differential scanning calorimetry.

## 2. Experimental

### 2.1. Materials

Peroxide cured HNBR sheets of 2mm thickness were prepared with the composition shown in Table 1. This composition was chosen to represent a typical HNBR that might be used in sealing applications in oilfield applications, and includes a base polymer which is 96% saturated with 36% acrylonitrile content. The HNBR used in this study also incorporates 50phr of HAF N-330 carbon black (26-30nm primary particle diameter [20]), which is routinely included in commercial products to increase mechanical properties, abrasion resistance and environmental stability. It has been shown that N-330 is not the optimum carbon black in terms of effectively reinforcing HNBR [21], and nanoplatelet type fillers can reinforce even more efficiently if dispersed and oriented appropriately [13, 14, 22, 23]. Therefore, this HNBR formulation was not designed to be the highest performing HNBR conceivable, but rather a HNBR which is representative of materials typically applied in subsea oilfield applications. After compounding, the HNBR was cured in 2mm thick sheets at 170°C for 20 minutes in a hot press, followed by 150°C for 4 hours in an oven. These curing parameters were selected based on curing studies performed by moving die rheometry immediately after compounding; these results are not included here. These sheets were then cut into specimen geometries for specific tests. The curing characteristics of the HNBR were measured by rheometry to verify that a high level of cure was achieved, however these results are not presented here.

**Table 1. Composition of the HNBR assessed in this paper.**

Material	phr
HNBR	100
Antioxidant	3
Stearic acid	0.5
Zinc Oxide	5
Magnesium Oxide	10

N-330 HAF Carbon Black	50
Plasticizer	20
Peroxide	10

## 2.2. Chemical Exposure

The samples (precut in the geometry required for post-exposure testing) were exposed to a hydrocarbon liquid phase (variation classification A.1.ii) with a gas phase (variation classification A.2.i), suggested by ISO 23936-2:2011 Annex A, and as shown here in Table 2. This exposure is designed to simulate ageing in a "sweet" chemical environment (i.e. without H<sub>2</sub>S) similar to that which might be encountered in sub-sea oil contacting equipment. Specimens were placed in pressure vessels at 100bar (~1450psi) at different temperatures for different time periods, as summarised in Table 3. The specimens were placed in a bespoke specimen holder to maintain the specimens in the centre of the pressure vessels, inside the hydrocarbon phase of the liquid mix, away from the walls and the floor of the vessel (see Figure 1). Different time ageing periods were achieved by removing some specimens at various times points, and re-pressurizing the pressure vessels with the remaining specimens inside. The temperature and pressure of the pressure vessels was recorded continuously during the filling, holding and depressurizing processes. After exposure, but before any testing, all specimens were allowed to dry in air at ambient temperature to allow evaporation of residual solvents until the rate of drying decreased to below 0.01% mass change per day, which was typically achieved in 7-14 days after removal

**Table 2.** Chemical environment for exposure of specimens.

Proportion of Total Volume	Proportion of Phase
30% gas	95% CH <sub>4</sub> 5% CO <sub>2</sub>
10% de-ionised water	-
60% organic liquid ("Test Solvent Mix")	70% Heptane 20% Cyclohexane 10% Toluene

**Table 3.** Specimen names identifying exposure conditions included in this study.

Exposure Time Exposure Temperature	1 Week	3 Weeks	6 Weeks	12 Weeks
130°C	130°C - 1W	130°C - 3W	130°C - 6W	130°C - 12W
140°C	140°C - 1W	140°C - 3W	140°C - 6W	140°C - 12W
150°C	150°C - 1W	150°C - 3W	150°C - 6W	150°C - 12W
160°C	160°C - 1W	160°C - 3W	160°C - 6W	160°C - 12W

### 2.3. Test Methods

#### 2.3.1. Mass of Specimens upon Removal from Chemical Exposure

In order to determine how much solvent had been absorbed by the tensile test specimens during exposure, the specimens were promptly weighed upon removal from the pressure vessels. Upon removal, the samples were dried on a paper towel to remove surface liquid and then weighed on a Mettler Toledo microbalance with readability of 0.1mg. The time between removal and the first measurement of mass is typically one hour.

#### 2.3.2. Tensile testing

Tensile tests were performed using a Zwick universal testing machine, fitted with a 2.5kN load cell and extensometer. Specimens were prepared by stamping them from a sheet material to test geometry described in ISO 37 type 2, before any chemical exposure. The specimens were loaded in tension until failure at a constant crosshead displacement rate of 25mm.min<sup>-1</sup> and a preload of 0.5N. The tensile modulus was calculated as the gradient of the stress vs. strain curve in the range of 0.05-0.25% strain, as measured by a Zwick Multiextens extensometer with an accuracy grade of 0.5 according to EN ISO 9513. At least four specimens were tested for each set of exposure conditions. All tensile tests were performed in ambient conditions.

#### 2.3.3. Dynamic Mechanical Analysis (DMA)

Dynamic mechanical analysis was performed using an Anton Paar MCR300 modular compact rheometer operating in torsional oscillation mode. Specimens were prepared by stamping them prior to any exposure from a sheet material to a geometry of approximately 2mm x 2mm x 50mm, although the test gauge length for DMA was 45mm. The specimens were cyclically loaded in torsion at strain amplitude of 0.1% and a frequency of 1Hz during a constant temperature ramp of 0.64K.min<sup>-1</sup> from -60°C to 180°C. This temperature ramp yielded a data collection interval of approximately 2K. It has been reported that HNBRs are highly sensitive to strain rate and heating rate [24]; in this work, the heating rate was constant and the results presented here are for a single strain rate. Preliminary tests (not presented here) included testing of specimens at various strain ranges and revealed that a strain amplitude of 0.1% was

a suitable strain range to test these specimens, and showed that the stress vs. strain response was linear in this region, and no variation of shear modulus resulting from the Payne Effect [20] was detectable. To focus the investigation on the behaviour of the most aged specimens, only the specimens exposed at 160°C were assessed in DMA.

#### 2.3.4. Differential Scanning Calorimetry (DSC)

DSC was performed using a Perkin Elmer DSC 8500 to determine the presence of thermal transitions. Samples were cut from used tensile specimens which had been previously exposed to the solvent exposure described earlier. A sample of approximately 8mg of each material was placed in a closed aluminium pan and held at -50°C for 10 minutes to reach equilibrium. Subsequently, the samples were heated at 20K/min from -50°C to 40°C. To focus the investigation on the behaviour of the most aged specimens, only the specimens exposed at 160°C were assessed in DSC.

### 3. Results and Discussion

#### 3.1. The Mass of Specimens upon Removal from Chemical Exposure

The specimens removed from the pressure vessels after chemical exposure in the water/test solvent mix shown in Table 2, were weighed shortly after removal to determine the weight gain due to absorption of the solvents during immersion. Subsequently, the samples were repeatedly weighed over time of drying in air. The percentage increase in specimen mass due to swelling is shown in Figure 2, as a function of drying time in air at ambient conditions. Note that the initial mass measurements were performed at approximately 1 hour after removal from the pressure vessels, in which time absorbed solvents were already evaporating from the specimens into the air. Therefore, these initial values of mass are an underestimate of the real swollen values of the HNBR specimens on removal from the pressure vessels.

The specimens exposed at 130°C show a 14% initial increase in mass (comparing the pre-exposure mass to the mass measured one hour after removal from the pressure vessel), followed by a decrease in mass due to solvent evaporation. All of these specimens exposed at 130°C show a similar mass loss (i.e. solvent drying) behaviour over time in air. The specimens exposed at 140°C show similar behaviour, but with slight a variation depending on exposure time. Specimens aged for 12 weeks at 140°C, show a slightly slower weight loss rate than the rest of the specimens exposed at 140°C. The specimens exposed at 150°C show a clear difference as a function of the exposure time, and the weight loss rate decreases with increasing exposure time. The specimens exposed at 160°C show an even clearer trend; the specimens exposed for 160°C for 12 weeks showed not only the greatest initial mass but also the slowest weight loss rate of all specimens. Even after circa  $10^4$  hours (>400 days) of drying in ambient air, the specimens do not return to their initial mass, and instead appear to have gained mass during the exposure. A possible explanation for this behaviour is that some of the test solvent mix absorbs into the HNBR in the early stages of exposure, but the increasing crosslink density due to material ageing over time prevents these chemicals from diffusing out

of the HNBR after it has been removed from the test solvent mix. Another possible contribution to this residual mass increase could be from water becoming chemically bound to, or physically entrapped in, the MgO filler, as reported by Han *et al.* [25]. The general reduction in drying rate with increasing degree of ageing suggests that increasing crosslinking restricts the mobility of the absorbed solvent, leading to slower movement of solvent through the HNBR to the surface where evaporation can occur.

### 3.2. Tensile Testing

Representative stress vs. strain curves for each of the groups of aged specimens are shown in Figure 3. Tests were performed on specimens whose proportional weight change (due to residual solvents evaporating in ambient air) had reached a rate of  $<0.01\%/day$ . A typical stress vs. strain curve of a virgin (unexposed) specimen is included in each graph for comparison. After ageing at  $130^{\circ}\text{C}$ , there is a small change in tensile behaviour; a small reduction in tensile stiffness is seen compared to the virgin specimen. This reduction in stiffness could be due to the effect of residual solvents from the ageing process remaining in the samples and having a plasticizing effect. Since the samples aged at  $130^{\circ}\text{C}$  show approximately the same behaviour regardless of ageing time, it is assumed that there is no effect of ageing time up to 12 weeks at  $130^{\circ}\text{C}$ . Specimens aged at  $140^{\circ}\text{C}$  show a similar behaviour except that the 12 week aged samples begin to show a difference in behaviour with some slight stiffening in the low strain region. Specimens aged at  $150^{\circ}\text{C}$  start to show stiffening behaviour from 3 weeks of exposure, since the  $150^{\circ}\text{C} - 3\text{W}$  specimens show similar behaviour to the virgin material, which, assuming the same softening effect as seen in  $130^{\circ}\text{C}$  and  $140^{\circ}\text{C}$  aged specimens, implies a stiffening of the material to compensate for this softening. Specimens aged at  $150^{\circ}\text{C}$  for 6 or 12 weeks show markedly different stress vs. strain behaviour. This effect is even more pronounced in the specimens aged at  $160^{\circ}\text{C}$ , with the most aged specimens ( $160^{\circ}\text{C} - 12\text{W}$ ) showing initial very high stiffness and subsequent yielding behaviour. It can be seen in Figure 3 that the specimens aged for 6 and 12 weeks at  $150^{\circ}\text{C}$  and for 3, 6 and 12 weeks at  $160^{\circ}\text{C}$  show very much different initial stiffness, but similar post yield stiffnesses as illustrated by (a), (b) and (c) in Figure 3. The average stiffnesses measured in the strain range of 0.05-0.25% strain are compared in Figure 4. This comparison of stiffness in this very low strain range (0.05-0.25% strain) is performed to compare the initial mechanical properties, although it is also relatively common to compare the stiffnesses of elastomers at higher (50% or 300%) strains. This is not performed here as Figure 3 revealed that the stress vs. strain curves for these different specimens varies greatly with exposure conditions and, therefore, such a comparison at an arbitrary strain is considered to have limited value. As described earlier, there is no significant change in stiffness of specimens aged at  $130^{\circ}\text{C}$ . Specimens aged at temperatures from  $140^{\circ}\text{C}$  and above show an increase in stiffness due to ageing. A comparison of the masses of the specimens before and after exposure showed that although the samples were considered to have reached a stable mass (i.e. a mass loss rate of  $<0.01\%/day$ ) before mechanical testing, all samples used for tensile testing showed a residual 4-10% mass increase compared to their pre-exposure masses. The

most aged specimens showed the greatest residual mass increase. It is assumed that this mass increase following ageing can be attributed to the presence of residual solvents due the ageing exposure. These residual solvents would be expected to plasticise the specimens, and thus these measurements probably give a slight underestimation of the tensile stiffness of the materials. This would be particularly true for the specimens which had experienced the highest exposure temperatures for the longest durations, since these showed the greatest mass increase resulting from the ageing exposure. The most heavily aged specimens (160°C – 12W) show an increase of stiffness of approximately 27x that of the virgin specimens. Therefore, a slight underestimation of stiffness due to residual solvents in the tensile specimens (as seen in the specimens aged at 130°C) is not considered significant compared to the large increases in stiffness that occur when specimens start to show ageing effects.

The average strains to failure of these specimens are shown in Figure 5. All aged specimens show reduced strain to failure following ageing, which as in the stress vs. strain curves in Figure 3, could be affected by some residual solvents remaining from the chemical exposure ageing process. Figure 5 suggests that specimens aged at 150°C and 160°C show similar strain to failure changes as function of ageing time. However, this should be considered in the context of Figure 3, which showed that these specimens exhibit very different overall tensile response, of which strain to failure is only one measure. Although it has been reported that changes in strain to failure may be a good indicator of the ageing process in some rubbers [26], in the materials analysed here, the change in shape of the stress vs. strain curves means that considering the strain to failure alone is not appropriate for these aged specimens.

Figure 6 shows the effect of the exposure on the tensile strength of the specimens. Although these data show that the strength is reduced after exposure, and not closely related to exposure time, the complete shape of the stress vs. strain curves shown in Figure 3 must again be considered. It is clear that even with low strain to failure, the very high stiffness of the most aged specimens (160°C-12W) means that these achieve a high tensile stress before failure. The fact that the full stress vs. strain curves show big differences between specimens, while the tensile strength graphs show much less difference demonstrates the risks associated with choosing an acceptability criterion for aging based only on one measure, rather than considering the general material behaviour from stress vs. strain curves.

It has been reported that an increase in saturation of the butadiene groups (i.e. decreasing the ratio of x:y shown in Figure 7) during thermal aging is also linked to an increase in the stiffness and decrease the strain to failure of similar HNBRs [8], both of which are seen in these samples reported here and, therefore, could be a contributing factor. However, as the HNBR used in this work is 96% saturated at the start of the exposure, it seems unlikely that further saturation can explain the large increase in stiffness. Additionally, although the HNBR was considered to be effectively cured during manufacture, it is also possible that incomplete curing during manufacture could be completed during the aging process, since the temperatures used during HNBR curing (150-170°C) are in the same range as the temperatures

used in the ageing exposure (130-160°C). Since the curing was determined to be complete by using post-production rheometry, further curing during exposure combined are also considered unlikely to cause such a large increase in tensile stiffness. Therefore, the most likely explanation is that additional chemical crosslinking is responsible for this increase in stiffness by inhibiting molecular movement during low strain deformation.

One application of HNBR is for sealing rings in joints in oilfield equipment. In such applications, the sealing ring must be able to deform and return to the original geometry as the joint is loaded and unloaded to maintain a seal and thus prevent leakage. Therefore, the compression set of the material, i.e. the ability to resist permanent deformation and return to the original geometry upon unloading, is likely to be strongly affected by such a dramatic increase in stiffness as a function of chemical aging. While the seal may perform adequately under constant loading even during ageing, a post-exposure stiffened sealing ring may not be able to return to the original geometry when the load is reduced, resulting in the loss of the seal and leakage past the stiffened, still-deformed sealing ring. Similarly, sealing rings which undergo cyclic pressurization must be able to withstand damage due to decompression of gases which are dissolved into the material during high pressure application. If the diffused gases in the polymer cannot diffuse out on depressurization of the material, their expansion causes internal cracks and tears of the polymer. The ability of a component to resist damage due to this rapid gas decompression (RGD) depends on the speed at which dissolved gases can diffuse out, but also the ability of the material to strain without plastic damage. The differing solvent evaporation rates shown in Figure 2, suggest that the movement of solvents through rubber network are strongly affected by ageing processes, and therefore RGD resistance would be expected to decrease over service life. This RGD resistance is also linked to the toughness of the material, and may be impacted by the large decreases in strain to failure as shown in Figure 5.

### 3.3. Dynamic Mechanical Analysis

Figure 8 shows the storage and loss moduli in shear,  $G'$  and  $G''$  respectively, and the loss ratios ( $\tan \delta$ ) of selected specimens aged at 160°C, as a function of analysis temperature. As expected, the virgin HNBR specimen shows a peak in  $\tan \delta$  at approximately -16°C, which is associated with glass transition temperature. This is in the range of other values reported in literature for similar HNBR compounds [1, 22, 27, 28]. The magnitude of the  $\tan \delta$  peak is seen to decrease with increasing exposure time, although the temperature of this transition is similar in specimens 160°C – 3W and 160°C – 6W. The most aged specimen, 160°C – 12W, shows a very small transition and very small peak in  $\tan \delta$  in this temperature region. The maximum of the  $\tan \delta$  of 160°C – 12W in this region is approximately 1°C, although the peak has become very broad so accurately determining a maximum is difficult. The measured peaks are presented in Table 4, which also includes a comparison with transition temperatures determined from DSC data, which will be discussed subsequently.

It was shown earlier that the static tensile modulus (measured at room temperature) of the most heavily aged specimens was much greater than the unaged specimens, and the increase in stiffness was linked to the ageing time at 160°C. The DMA results here suggest that all of the specimens have similar shear moduli below  $T_g$ , but the degree of increase of molecular mobility which defines  $T_g$  is reduced following ageing. The assumption, therefore, is that, during the chemical exposure, an increase in apparent crosslink density occurs which does not significantly affect the sub- $T_g$  performance (where molecular mobility is restricted anyway), but inhibits the molecular mobility such that even above the expected  $T_g$ , the molecular mobility continues to be restricted. As the glass transition temperature is only slightly shifted in temperature, but greatly reduced in intensity, it is likely that these crosslinks are chemical crosslinks. The exact nature of these newly formed crosslinks is not investigated further here, but they are probably either imide (as proposed by Tripathy and Smith [29, 30]) or ketimine (as proposed by Bhattacharjee et al. [7]) type crosslinks formed from attack of the acrylonitrile groups (see Figure 9), and discussed further by Bender and Campomizzi [8]. It is also worth noting that these mechanisms would probably be different during exposure to a "sour" ( $H_2S$  containing) ageing environment [16]. Although these mechanical results do suggest increased crosslinking, there is no definitive indication of the degree of chain scission that may be occurring during these aging processes. NMR studies reported in literature suggest that different unfilled HNBRs exposed hot air aging did not appear to undergo significant chain scission [5], but these results are only indicative as they were for specimens aged at lower temperatures and shorter time scales than considered in this research.

### 3.4. DSC

Figure 10 shows DSC analyses of virgin HNBR and HNBR specimens which had been aged for 3, 6 and 12 weeks at 160°C. These results show a thermal transition in the virgin HNBR in the region of -20°C, which is similar to the  $T_g$  of the HNBR measured by DMA. It has been reported that glass transition temperature generally increases with acrylonitrile content [31], and a single endothermic step is typically reported for other HNBRs [21, 32, 33]. As seen previously in dynamic mechanical data (see Figure 8), the magnitude of this transition decreases with increasing exposure time, until it is barely detectable in the sample which had been exposed at 160°C for 12 weeks. Differentiation of these curves revealed the midpoints of these transition steps to decrease from -21.2°C in the virgin material to ca. -15°C in the specimen that has been aged at 160°C for 12 weeks. As shown in Figure 10, the thermal transition of the specimen that has been aged at 160°C for 12 weeks is very slight and, therefore, a peak is difficult to quantify with high precision using DSC.

**Table 4.** Transition temperature determination from DMA (peak of first differential of storage modulus and peak of tan delta) and DSC data (midpoint of endotherm step).

Specimen	DMA (see Figure 8)	DSC (see Figure 10)
----------	-----------------------	------------------------

	Midpoint of G' Step	Peak G''	Peak tan $\delta$	Midpoint of endotherm step
Virgin	-19.7°C	-19.8°C	-15.6°C	-21.2°C
160°C – 3W	-19.4°C	-18.3°C	-13.0°C	-20.4°C
160°C – 6W	-17.0°C	-17.2°C	-12.8°C	-18.6°C
160°C – 12W	-5.2°C	-6.2°C	1°C	approx. -15°C

#### 4. Conclusions

The HNBR compounds reported here undergo a large increase in tensile stiffness and reduction in strain to failure when exposed to mixed hydrocarbon fluids at elevated temperatures and pressures. This would certainly impact the sealing performance and rapid gas decompression resistance of these materials if they experienced similar exposure conditions in service. The exact mechanisms are not explored in this paper, but are attributed to an increase in apparent crosslink density, most probably due to new chemical crosslinks resulting from attack of the acrylonitrile groups. Although failure values (tensile strength and strain to failure) may be used to assess the degree of ageing of polymers, these should always be seen in the context of the shape of the stress vs. strain curves. In the case of the HNBR compounds analysed here, the shape of the stress vs. strain curves changed considerably after chemical ageing, and tensile strength alone was not considered a clear indicator of the change in performance.

Gravimetric studies of the swollen specimens after removal from the hydrocarbon mix showed that the more aged specimens dried significantly more slowly than less aged specimens. Dynamic mechanical analysis and calorimetry showed a decrease in the magnitude of the glass transition with increasing aging, suggesting that the segmental mobility which would normally increase at the glass transition temperature is restricted by the proposed increase in additional crosslinks formed during ageing.

#### 5. Acknowledgements

This work is part of the collaborative project “PolyLife” with the industrial partners FMC Kongsberg Subsea AS, Kongsberg Oil & Gas Technologies AS, Roplast GmbH, Petróleo Brasileiro SA and the research institutes Norwegian University of Science and Technology (NTNU) and SINTEF Materials and Chemistry. The authors would like to express their thanks for the financial support by The Research Council of Norway (Project 193167 in the Petromaks programme).

1. Wrana, C., K. Reinartz, and H.R. Winkelbach, *Therban® – The High Performance Elastomer for the New Millennium*. Macromolecular Materials and Engineering, 2001. **286**(11): p. 657-662.
2. Mohammed, M.H., et al., *Physical properties of poly(ether ether ketone) exposed to simulated severe oilfield service conditions*. Polymer Degradation and Stability, 2013. **98**(6): p. 1264-1270.
3. Knörger, M., et al., *Spatially resolved and integral NMR investigation of the aging process of carbon black filled natural rubber*. Polymer Bulletin, 1997. **38**(1): p. 101-108.
4. Garbarczyk, M., et al., *Characterization of aged nitrile rubber elastomers by NMR spectroscopy and microimaging*. Polymer, 2002. **43**(11): p. 3169-3172.
5. Chaudhry, R.A., et al., *Influence of molecular parameters and processing conditions on degradation of hydrogenated nitrile butadiene rubbers*. Journal of Applied Polymer Science, 2005. **97**(4): p. 1432-1441.
6. Gent, A.N., *Engineering with Rubber*. 2001: Hanser.
7. Bhattacharjee, S., A.K. Bhowmick, and B.N. Avasthi, *Degradation of hydrogenated nitrile rubber*. Polymer Degradation and Stability, 1991. **31**(1): p. 71-87.
8. Bender, H. and E. Campomizzi, *Improving the heat resistance of hydrogenated nitrile rubber compounds. Part 1: Aging mechanisms for high saturation rubber compounds*. Kautschuk Gummi Kunststoffe, 2001. **54**(1): p. 14-21.
9. Chen, S., et al., *Thermal degradation behavior of hydrogenated nitrile-butadiene rubber (HNBR)/clay nanocomposite and HNBR/clay/carbon nanotubes nanocomposites*. Thermochimica Acta, 2009. **491**(1-2): p. 103-108.
10. Bystritskaya, E.V., T.V. Monakhova, and V.B. Ivanov, *TGA application for optimising the accelerated aging conditions and predictions of thermal aging of rubber*. Polymer Testing, 2013. **32**(2): p. 197-201.
11. Thavamani, P., et al., *The effect of crosslink density, curing system, filler and resin on the decomposition of hydrogenated nitrile rubber and its blends*. Thermochimica Acta, 1993. **219**(0): p. 293-304.
12. Linde, E., et al., *Long-term performance of a DEHP-containing carbon-black-filled NBR membrane*. Polymer Testing, 2014. **34**: p. 25-33.
13. Choudhury, A., et al., *Effect of Various Nanofillers on Thermal Stability and Degradation Kinetics of Polymer Nanocomposites*. Journal of Nanoscience and Nanotechnology, 2010. **10**(8): p. 5056-5071.
14. Cadambi, R.M. and E. Ghassemieh, *The ageing behaviour of hydrogenated nitrile butadiene rubber/nanoclay nanocomposites in various mediums*. Journal of Elastomers and Plastics, 2012. **44**(4): p. 353-367.
15. Campomizzi, E.C., H. Bender, and W. von Hellens, *Improving the heat resistance of Hydrogenated nitrile rubber compounds. Part 2: Effect of a novel heat stabilizer additive on the heat resistance of HNBR*. Kautschuk Gummi Kunststoffe, 2001. **54**(3): p. 114-121.
16. Cong, C., et al., *Degradation of hydrogenated nitrile-butadiene rubber in aqueous solutions of H<sub>2</sub>S or HCl*. Chemical Research in Chinese Universities, 2013. **29**(4): p. 806-810.
17. Smith, K.C. and B.S. Tripathy, *HNBR and long term serviceability in automotive lubricants: Structure property relationships* in *Rubber World*. 1998. p. 28-45.
18. Wise, J., K.T. Gillen, and R.L. Clough, *An ultrasensitive technique for testing the Arrhenius extrapolation assumption for thermally aged elastomers*. Polymer Degradation and Stability, 1995. **49**(3): p. 403-418.
19. Champion, R.P. *Model Test 'Oils' Based on Solubility Parameters for Artificial Ageing of Polymers*. in *Polymer Testing '96. The Second International Conference on the Testing of Polymers*. 1996. UK: RAPRA.

20. Donnet, J.-B. and E. Custodero, *Reinforcement of Elastomers by Particulate Fillers*, in *The Science and Technology of Rubber*, J.E. Mark, B. Erman, and C.M. Roland, Editors. 2013, Elsevier.
21. Šebenik, U., et al., *Dynamic mechanical properties and structure of in situ cured polyurethane/hydrogenated nitrile rubber compounds: Effect of carbon black type*. *Journal of Applied Polymer Science*, 2012. **125**(S1): p. E41-E48.
22. Gatos, K.G., et al., *Nanocomposite Formation in Hydrogenated Nitrile Rubber (HNBR)/Organo-Montmorillonite as a Function of the Intercalant Type*. *Macromolecular Materials and Engineering*, 2004. **289**(12): p. 1079-1086.
23. Gatos, K.G., et al., *Controlling the Deintercalation in Hydrogenated Nitrile Rubber (HNBR)/Organo-Montmorillonite Nanocomposites by Curing with Peroxide*. *Macromolecular Rapid Communications*, 2005. **26**(11): p. 915-919.
24. Likozar, B. and M. Krajnc, *Temperature Dependent Dynamic Mechanical Properties of Hydrogenated Nitrile Butadiene Rubber and the Effect of Peroxide Cross-linkers*. *e-Polymers*, 2007. **7**(1): p. 1536-1555.
25. Han, D., et al., *Swellable elastomeric HNBR–MgO composite: Magnesium oxide as a novel swelling and reinforcement filler*. *Composites Science and Technology*, 2014. **99**(0): p. 52-58.
26. Bystritskaya, E.V., A.L. Pomerantsev, and O.Y. Rodionova, *Evolutionary design of experiment for accelerated aging tests*. *Polymer Testing*, 2000. **19**(2): p. 221-229.
27. Shi, X., et al., *HNBR/EPDM blends: Covulcanization and compatibility*. *Journal of Applied Polymer Science*, 2013. **129**(5): p. 3054-3060.
28. Hornig, K. and K. Athanasopulu, *Betrachtung von Löslichkeitsparametern zur Beschreibung der Elastomer-Weichmacherkompatibilität am Beispiel von HNBR – Teil 1. (Examination of solubility parameters to characterise the elastomer-plasticiser compatibility using the example of HNBR – Part 1)*. *Kautschuk Gummi Kunststoffe*, 2011. **64**(3): p. 165-175.
29. Tripathy, B.S. and K.C. Smith, *HNBR and Long Term Serviceability in Modern Automotive Lubricants. Part I: Analytical Study*, in *152nd Fall Technical Meeting of the Rubber Division, American Chemical Society*. 1997: Cleveland, Ohio, USA.
30. Smith, K.C. and B.S. Tripathy, *HNBR and Long Term Serviceability in Modern Automotive Lubricants. Part II: Structure Property Relationships*, in *152nd Fall Technical Meeting of the Rubber Division, American Chemical Society*. 1997: Cleveland, Ohio, USA.
31. Severe, G. and J.L. White, *Physical properties and blend miscibility of hydrogenated acrylonitrile-butadiene rubber*. *Journal of Applied Polymer Science*, 2000. **78**(8): p. 1521-1529.
32. Yeo, Y.-G., H.-H. Park, and C.-S. Lee, *A study on the characteristics of a rubber blend of fluorocarbon rubber and hydrogenated nitrile rubber*. *Journal of Industrial and Engineering Chemistry*, (0).
33. Severe, G. and J.L. White, *Transition behaviour of hydrogenated acrylonitrile-butadiene rubber*. *Kautschuk Gummi Kunststoffe*, 2002. **55**(4): p. 144-148.

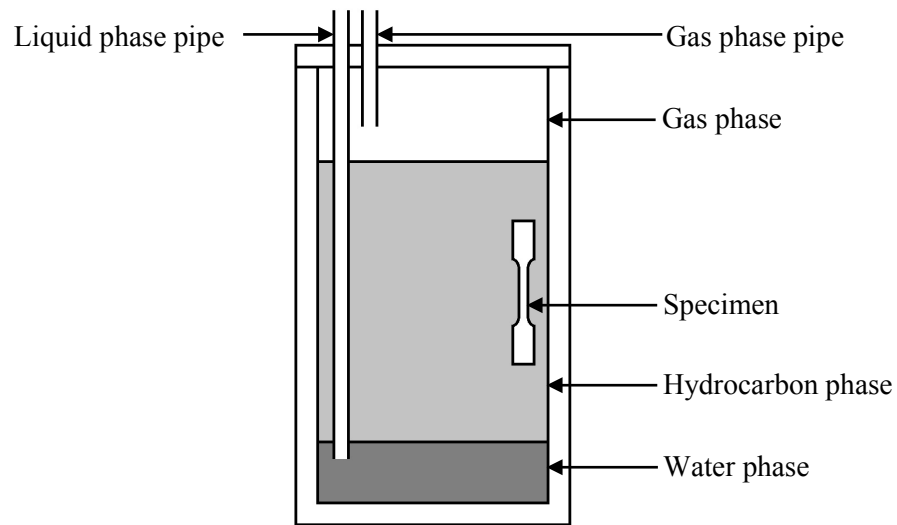


**Figure 1.** Schematic of pressure vessel used for chemical exposure of the specimens. The specimens are held in the hydrocarbon phase by a specimen holder (not shown in this schematic). Thermocouple and manometer are also present in the experimental set-up but not shown in this schematic.

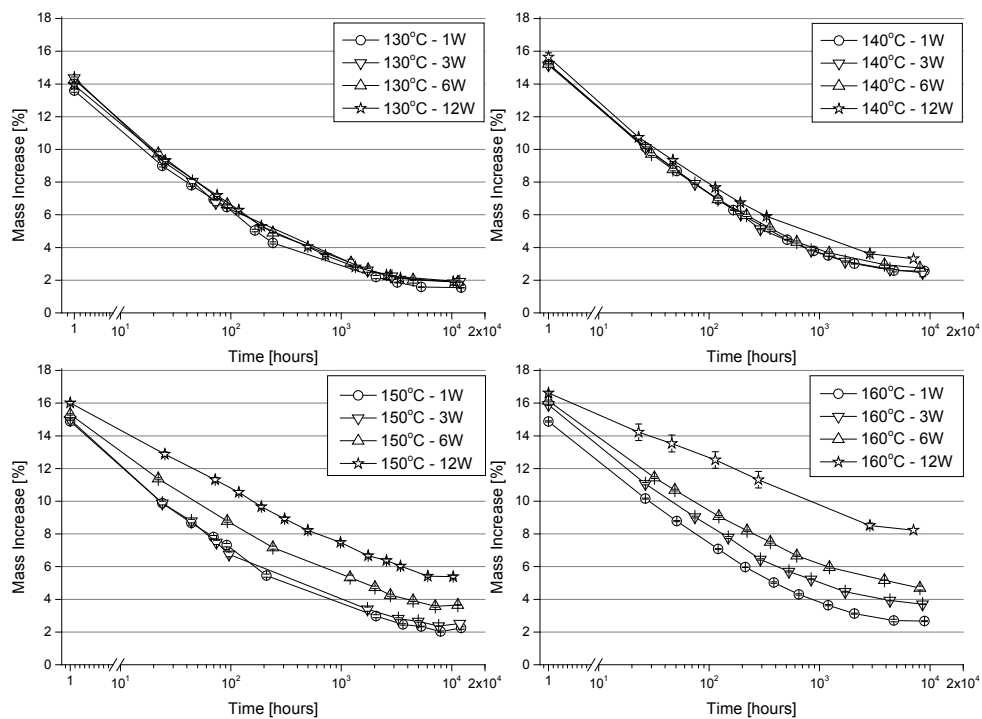


**Figure 2.** Mass change over time following initial mass increase during ageing and subsequent decrease due to evaporation in air, following exposure in pressure vessels at 130°C, 140°C, 150°C and 160°C for 1, 3, 6 and 12 weeks. Note that on first removal from the pressure vessels, the mass is 14-17% greater than before exposure (depending on ageing conditions), and the mass increase decreases with time in air due to evaporation of absorbed solvents.

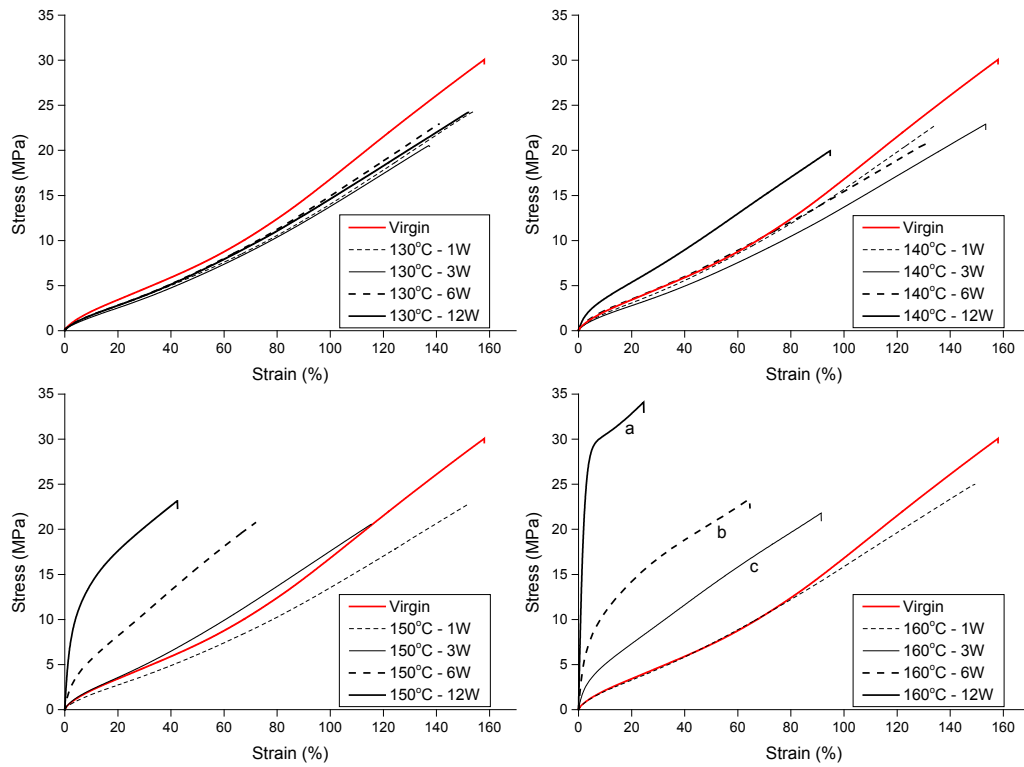


**Figure 3.** Typical stress vs. strain curves for specimens subjected to each of the ageing conditions, compared to a virgin (unaged) specimen. Axes are consistent in all of these graphs to aid comparison. Top-left: 130°C, top-right: 140°C, bottom-left: 150°C and bottom-right: 160°C.

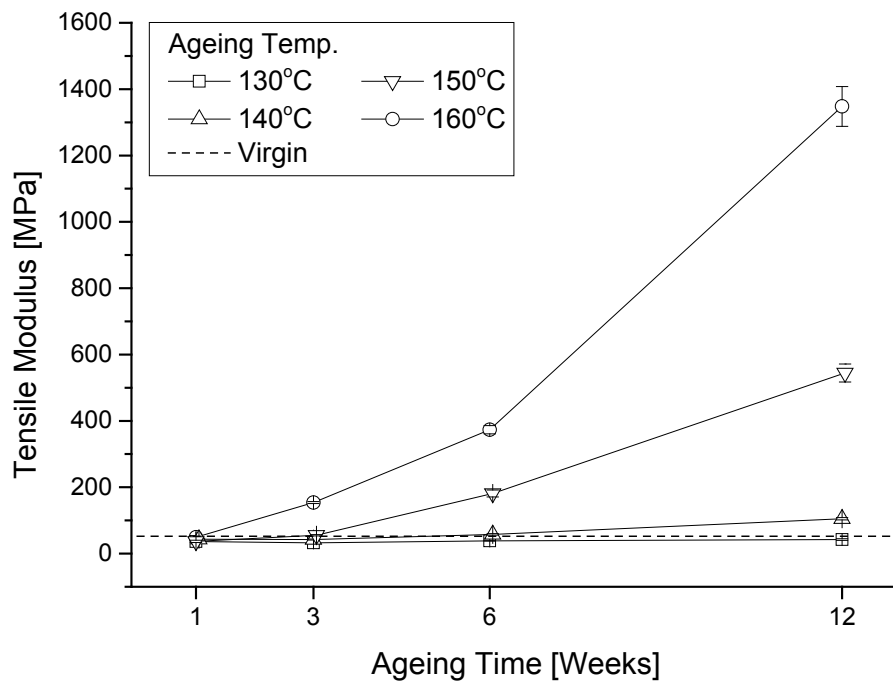


**Figure 4.** Tensile modulus of specimens after having been aged at different temperatures. All tensile tests were performed at room temperature. Data points represent averages of at least four specimens per point, and error bars show standard deviation.

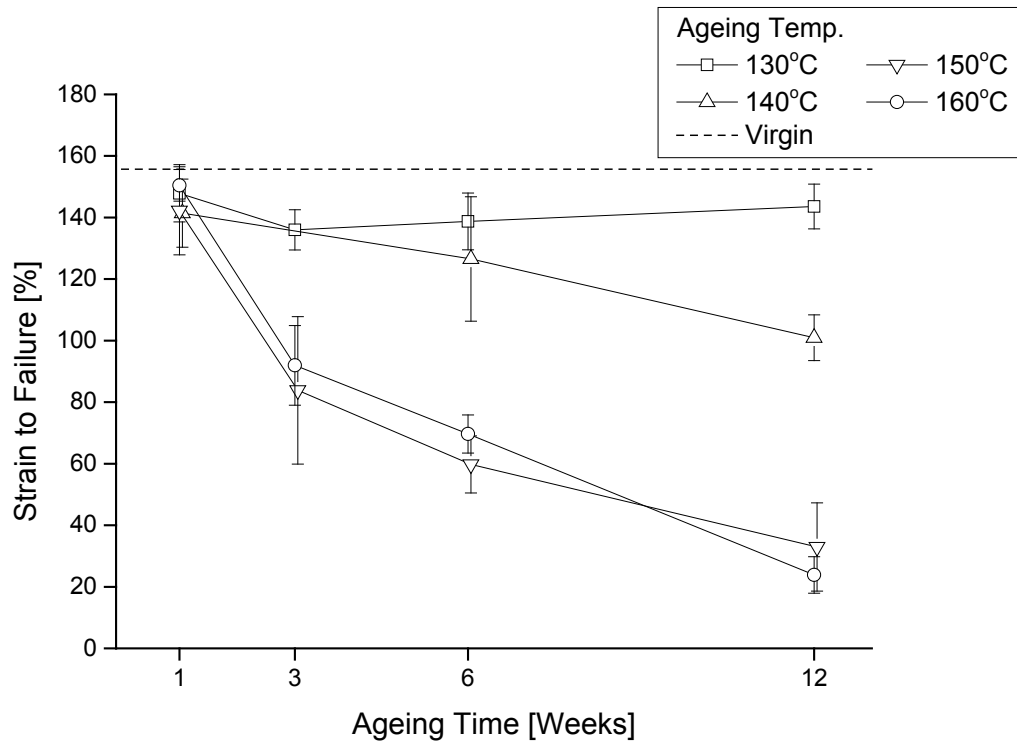


**Figure 5.** Strain to failure of specimens aged at different temperatures. Data points represent averages of at least four specimens per point, and error bars show standard deviation. Where error bars overlap, data points are shifted by small increments in the x-axis for clarity.

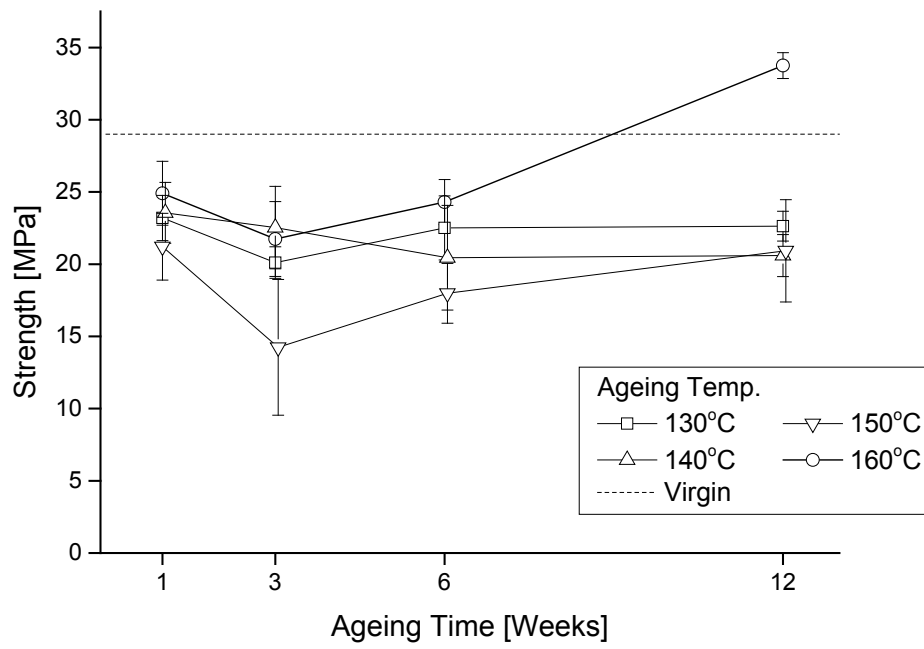


**Figure 6.** Tensile strength of specimens aged at different temperatures. Data points represent averages of at least four specimens per point, and error bars show standard deviation. Where error bars overlap, data points are shifted by small increments in the x-axis for clarity.

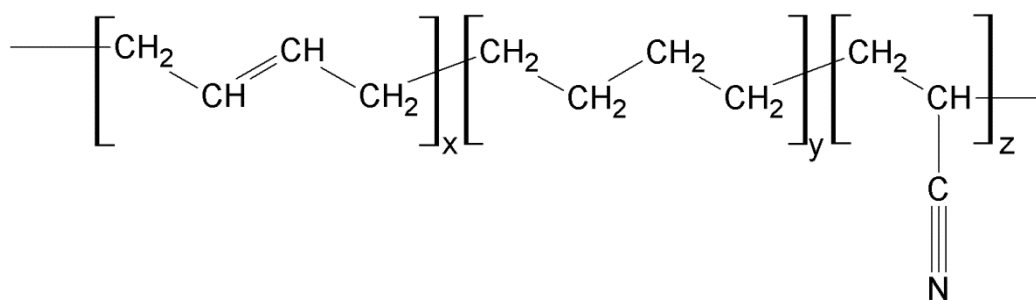


**Figure 7.** Simplified models of the structure of hydrogenated nitrile butadiene rubber (HNBR), with the ratio  $x:y$  indicating degree of saturation (residual double bonds), and  $z:(x+y)$  indicating the acrylonitrile content. In reality, many HNBRs do not have full saturation of the butadiene groups; the HNBR used in this paper is specified to be 96% saturated. Cis- and trans-isomers, pendant ethyl groups and branching of the butadiene are also present in HNBRs in reality, but not shown in this simplified model.

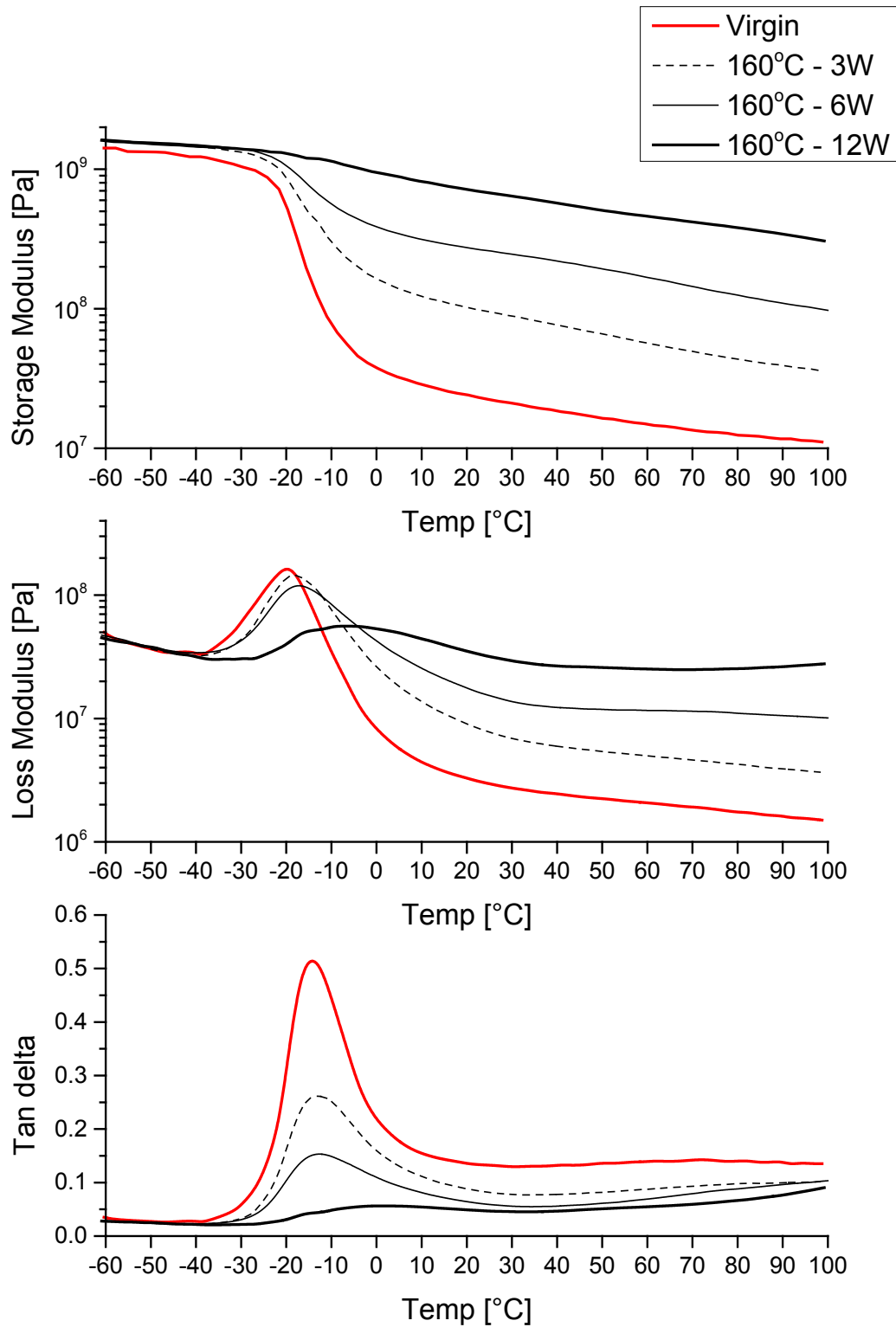


**Figure 8.** Storage modulus, ( $G'$ ), loss modulus ( $G''$ ) and tan delta of specimens subjected to exposure at 160°C for durations of 3, 6 and 12 weeks, compared to a virgin (unaged) specimen. Note that with increasing exposure time at 160°C, the tan delta peak decreases in height and the effect of increasing DMA temperature on  $G'$  decreases with increasing ageing temperature so that the most aged specimen (160°C – 12W) shows only a very small decrease in  $G'$  and a very small peak in tan delta at this temperature where a glass transition would be expected.

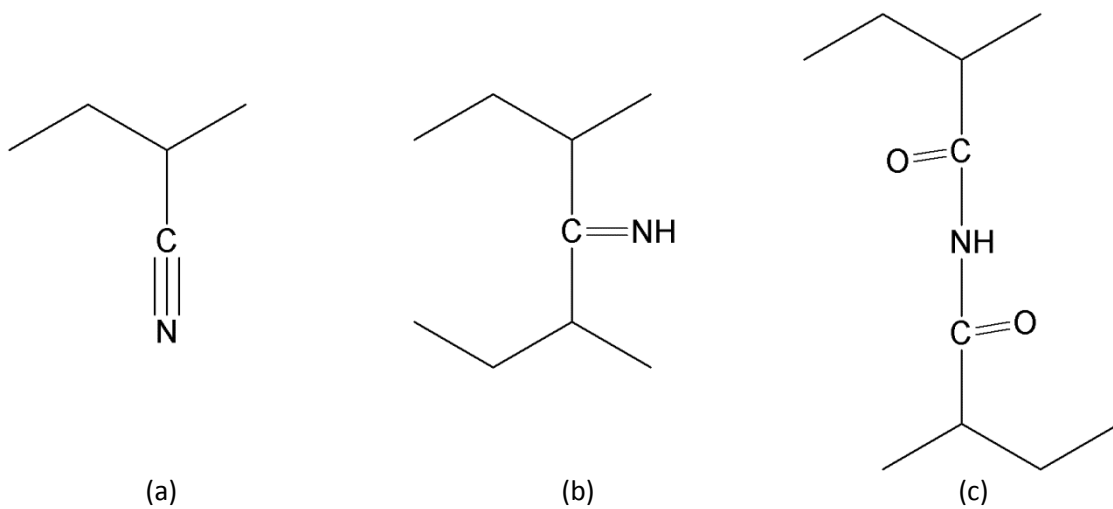


**Figure 9.** Some possible crosslinking mechanisms of the acrylonitrile group of HNBR during ageing in a sweet environment, as reported in literature. (a) the acrylonitrile group of HNBR (see also Figure 7) (b) a ketamine type crosslink [7], and (c) an imide type crosslink [30, 31].

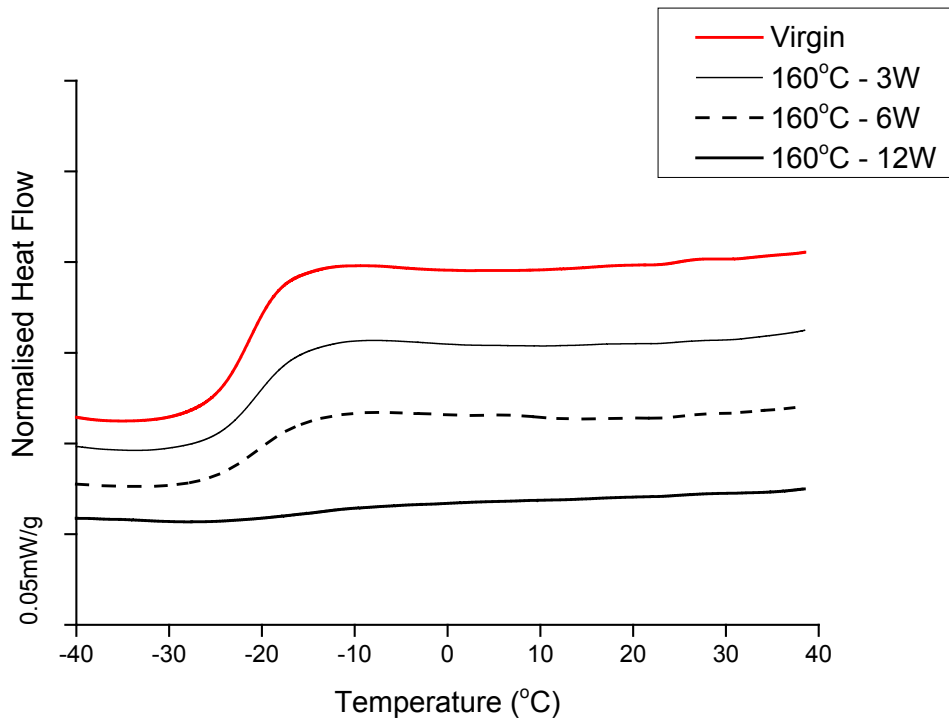


**Figure 10.** DSC results from samples aged in the test solvent mix; heat flow is normalized per unit mass of specimen, oriented with endotherms up. Curves are shifted in the y-axis for ease of comparison. The virgin specimen shows a significant thermal transition at approximately  $-21^{\circ}\text{C}$ , and the magnitude of this transition decreases with increasing ageing time until it is barely detectable in specimens which have been exposed to the solvents for 12 weeks.